17. ANTHROPOGENIC INTENSIFICATION OF SOUTHERN AFRICAN FLASH DROUGHTS AS EXEMPLIFIED BY THE 2015/16 SEASON

Xing Yuan, Linying Wang, and Eric F. Wood

Flash drought over southern Africa was tripled during the last 60 years mainly due to anthropogenic climate change, and it was intensified during 2015/16 in the midst of heat waves.

Introduction. Droughts are mainly driven by natural climate variability. They usually evolve slowly and persist for a few months to decades. Anthropogenic climate change, however, not only increases the likelihood of local and regional droughts, but also alters their characteristics (Sheffield and Wood 2008; Dai 2013; Trenberth et al. 2014). For instance, the soil moisture drought during growing seasons is often accompanied by heat waves, resulting in a type of drought that has a rapid onset and short duration (from a few days to 1–2 months), but high intensity and devastating impacts, which is recently termed "flash drought" (Hoerling et al. 2014; Mo and Lettenmaier 2015; Yuan et al. 2015; Wang et al. 2016). During November–April of 2015/16, most parts of southern Africa (SA; 10°–40°E, 10°–35°S) experienced a rainy season–long drought. Within the seasonal drought, heat waves occurred suddenly, which caused a severe flash drought characterized by soil moisture deficit and heat waves at the beginning of December. The flash drought was then terminated by a rainfall event in early January. The South African Weather Service announced that 32 daily temperature records were broken in South Africa with the highest reaching 45°C. Millions of people were affected by famine, disease, and water shortages. The SA drought is basically associated with the 2015/16 strong El Niño (Nicholson and Entekhabi 1986; Reason and Jagadheesha 2005; Yuan et al. 2013; Ratnam et al. 2014; Hoell et al. 2015) and possibly altered by Indian Ocean sea surface temperature variability (Reason 2001; Washington and Preston 2006; Manatsa et al. 2011; Hoell et al. 2016), but the warming climate may also play an important role. This study will investigate the 2015/16 SA flash drought in the context of a changing climate during 1948–2016, and detect the anthropogenic influences.

AFFILIATIONS: Yuan—Key Laboratory of Regional Climate-Environment for Temperate East Asia, Institute of Atmospheric Physics, Chinese Academy of Sciences, Beijing, China; Wang—Key Laboratory of Regional Climate-Environment for Temperate East Asia, Institute of Atmospheric Physics, Chinese Academy of Sciences, Beijing, and University of Chinese Academy of Sciences, Beijing, China; Wood—Department of Civil and Environmental Engineering, Princeton University, Princeton, New Jersey

DOI:10.1175/BAMS-D-17-0077.1

A supplement to this article is available online (10.1175/BAMS-D-17-0077.2.)

Data and methods. Daily precipitation and surface air temperature hybrid reanalysis–observational datasets at 0.25° resolution during 1948–2008 were obtained from Princeton's African drought monitoring and forecasting system (PADMF; Sheffield et al. 2014; Yuan et al. 2013). They were extended to 2016 by using NOAA's Climate Prediction Center (CPC) global 0.5° analysis of daily gauge measurements of precipitation (Chen et al. 2008) and ERA-Interim reanalysis of surface air temperature (Dee et al. 2011). Both CPC precipitation and ERA-Interim temperature were interpolated into 0.25° and were adjusted to match the climatology of the PADMF forcing data. The 500-hPa geopotential height data was also obtained from ERA-Interim reanalysis.

The Variable Infiltration Capacity (VIC; Liang et al. 1996) land surface hydrological model, which was calibrated against streamflow observations from over 800 Global Runoff Data Centre gauges before being implemented in the PADMF system (Yuan et al. 2013), was used in this study to estimate soil moisture. Driven by the meteorological forcings mentioned above, the VIC model was run from 1948 to 2016 over SA with default initial conditions, and the model states at the end of the run were used as initial conditions on 1 January 1948 for another 69-year simulation. Soil moisture from the second round simulation was used for the flash drought analysis.

Daily surface air temperature and soil moisture were aggregated into pentad-mean values for each 0.25° grid cells over SA during the growing seasons

(October–March). For each grid and each pentad, a flash drought is defined as pentad-mean surface air temperature anomaly is larger than one standard deviation, the percentile of target pentad-mean soil moisture is lower than 40%, and the soil moisture percentile of target pentad is at least 10% lower than the preceding pentad. A common view of droughts is a condition of land surface soil moisture deficits that accumulates gradually, while the third criterion of flash drought guarantees a remarkable swiftness. If two or more consecutive flash drought pentads happen one after another, they will be treated as a single drought event. The selection of the thresholds will be discussed below.

Daily precipitation and surface air temperature simulations from 13 atmosphere–ocean coupled general circulation models (CGCMs; see Table ES17.1 for the model list) provided by the Coupled Model Intercomparison Project Phase 5 (CMIP5; Taylor et al. 2012) were used in this study. Actually simulations of 30 CMIP5 models that combined anthropogenic and natural forcings (ALL) were used to drive the VIC land surface hydrological models, and 13 of them were selected according to their performance for flash drought changes, as well as data availability for the simulations that only considered natural forcing (NAT) or be controlled to preindustrial situations (CTL). CMIP5 simulated daily surface air temperature and CMIP5/VIC simulated daily soil moisture were used to identify flash drought events with or without anthropogenic forcings. In this study, CMIP5 NAT experiments covered the period 1950–2012, and CMIP5 ALL experiments were extended to 2016 by using model simulations under the representative concentration pathways (RCP) 4.5 emission scenario during 2006–16, which is a common way to extend the ALL experiments (Sun et al. 2014). The optimal fingerprint method (Allen and Stott 2003) was used to detect the anthropogenic influence on the change in flash drought over SA. In this study, the regression was conducted over 1961–2012 for two-signal ALL-NAT (ANT) and NAT analysis on non-overlapping 3-year averages of SA areal mean flash drought events by using the total least squares method.

Results. Figure 17.1a shows that extremely high regional mean temperature anomaly (2.85 standard deviations higher than the climatological mean) occurred during December 2015–January 2016, which was ranked as the highest since 1948. Meanwhile, there was also a severe rainfall deficit (one standard deviation lower than the climatology), although not the most severe in the history. Based on Mann–Kendall nonparametric trend analysis, it is found that both the decreasing trend in precipitation (–28.6 mm decade^{-1}) and increasing trend in temperature (+0.062°C decade^{-1}) are significant during 1948–2016, with statistical significances of $p < 0.05$ and $p < 0.01$, respectively. At the end of November 2015, there were deficits in the precipitation and soil moisture, but temperature was normal (Fig. 17.1b). However, the extremely high temperature anomaly (higher than one standard deviation) occurred at the beginning of December 2015 and lasted until the second pentad of January 2016, with precipitation lower than climatology by more than half standard deviation, and soil moisture percentile lower than 5% for a large area of SA (Figs. 17.1c–e). From the third pentad of January 2016, the rainfall events terminated the heat wave and alleviate the soil dryness to some extent (Fig. 17.1f).

It is possible that the dry soil triggered the heat waves (Mueller and Seneviratne 2012) and sustained them for the flash drought with such a long duration. Moreover, recent study found that the variability in Botswana High has a close relationship with rainfall and temperature anomalies over SA (Driver and Reason 2017). Figure 17.1a shows that the 500 hPa geopotential height averaged over the region has a positive correlation with temperature ($r = 0.71$) and a negative correlation with precipitation ($r = -0.38$), both are statistically significant. During 2015/16 austral summer, the height is almost 3 standard deviations higher than normal (Fig. 17.1a), which is also responsible for the drought and heat conditions.

Figure ES17.1a shows that the eastern part of SA (which is more humid) has a higher chance to experience flash drought than the western part. Other thresholds for the soil moisture percentile (e.g., 30%, 50%) and declining rate (e.g., 5% decline between two pentads) were tested, and similar spatial patterns were obtained with different magnitudes (Figs. ES17.1b,c). On average, flash drought events over SA increased by 220% from 1961 to 2016, with a significance level of $p < 0.01$ (black lines in Fig. 17.2a). The CMIP5/VIC ensemble simulations driven by all forcings (ALL) successfully captured this upward trend with $p < 0.01$ (red lines in Fig. 17.2a), but those with natural only forcing (NAT) had a very small upward trend (blue lines in Fig. 17.2a). This suggests that anthropogenic climate change is mainly responsible for the increasing flash drought over SA. The simulations of surface air temperature change are more reliable than those for soil moisture and precipitation (Figs. 17.2b,c), indicating the major source of uncertainty in detecting

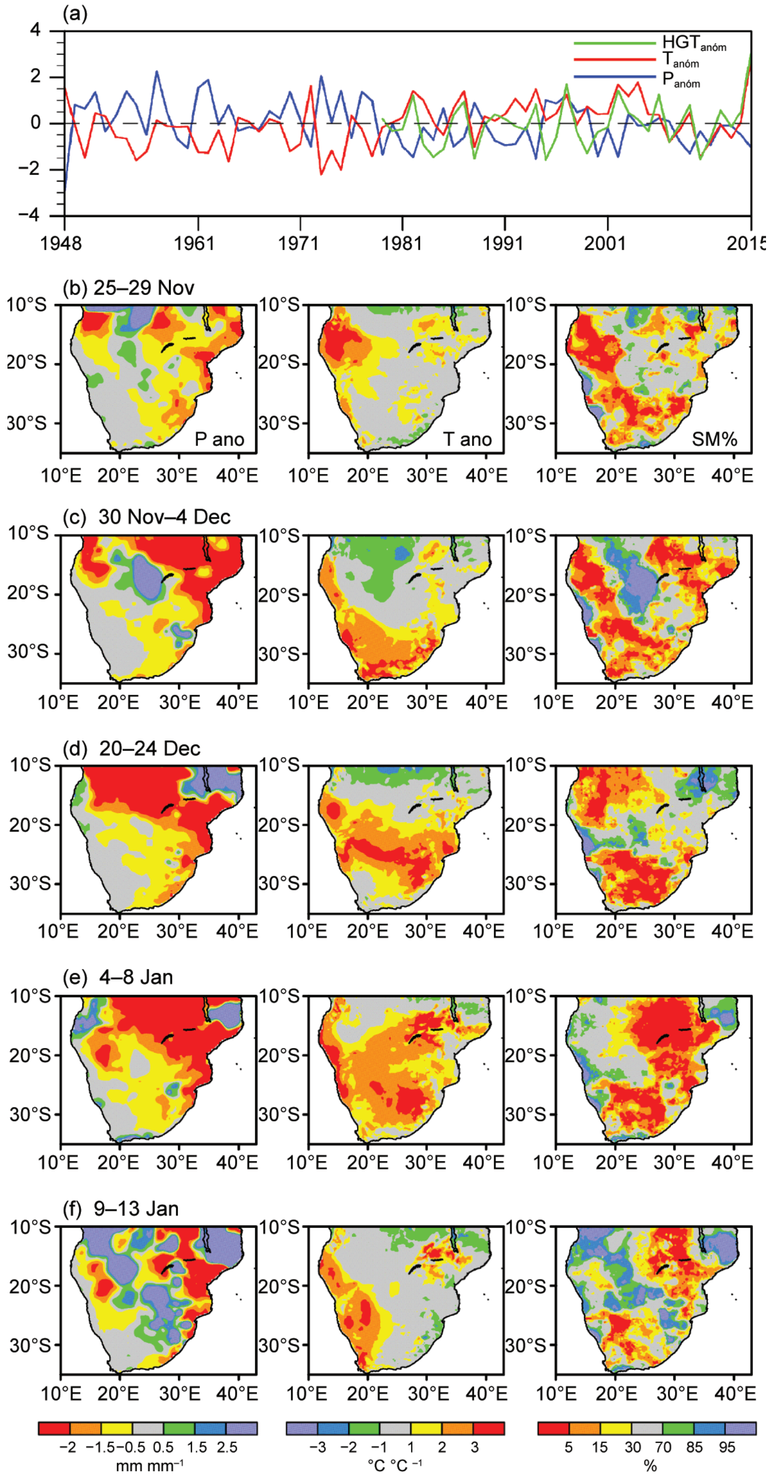

Fig. 17.1. (a) Interannual variations of standardized Dec–Jan mean precipitation (blue), temperature (red) and 500-hPa geopotential height (green) anomalies averaged over southern Africa (10°–40°E, 10°–35°S) during 1948–2016. (b)–(f) Flash drought snapshots of standardized pentad-mean precipitation (left; mm mm^{-1}) and surface air temperature (middle; °C °C^{-1}) anomalies and soil moisture percentiles (right; %) during Dec–Jan 2015/16. Precipitation and temperature anomalies were divided by std. dev. of the 1961–2012 climatology.

and attributing flash drought change is the soil moisture variation.

The best estimates of scaling factors show that both the anthropogenic and natural signals are detectable with $p < 0.01$ (Fig. 17.2e). As the NAT simulations do not have discernible upward trend in flash drought (Fig. 17.2a), the observed increasing flash drought over SA is mainly attributable to anthropogenic forcing (Fig. 17.2e). Therefore, although the recent strong El Niño as well as the high pressure anomaly have caused the 2015/16 drought conditions over SA, the warming climate may quite likely be responsible for the increasing likelihood of such severe flash drought.

Conclusions. A flash drought characterized by severe heat waves and soil moisture deficit hit southern Africa (SA) during December–January 2015/16, which raises the attention of flash drought risk over semihumid and semiarid regions. Similar to other parts of the world (Mazdiyasni and AghaKouchak 2015; Wang et al. 2016), there is a substantial increase in concurrent droughts and heatwaves in SA, with flash drought increased by 220% from 1961 to 2016. Although both the anthropogenic and natural signals are detectable in attributing the flash drought changes, the anthropogenic influence is mainly responsible for the increasing flash drought over SA. In the midst of heat waves, the risk of flash drought over SA is very likely to increase in the future.

ACKNOWLEDGMENTS. We would like to thank Dr. Martin Hoerling, Dr. Andrew Hoell, and two anonymous reviewers for their helpful comments. We acknowledge the World Climate Research Programme's Working Group on Coupled Modeling, which is responsible for CMIP. This work was supported by National Key R&D Program of China (2016YFA0600403), National Natural Science Foundation of China (91547103), China Special Fund for Meteorological Research in

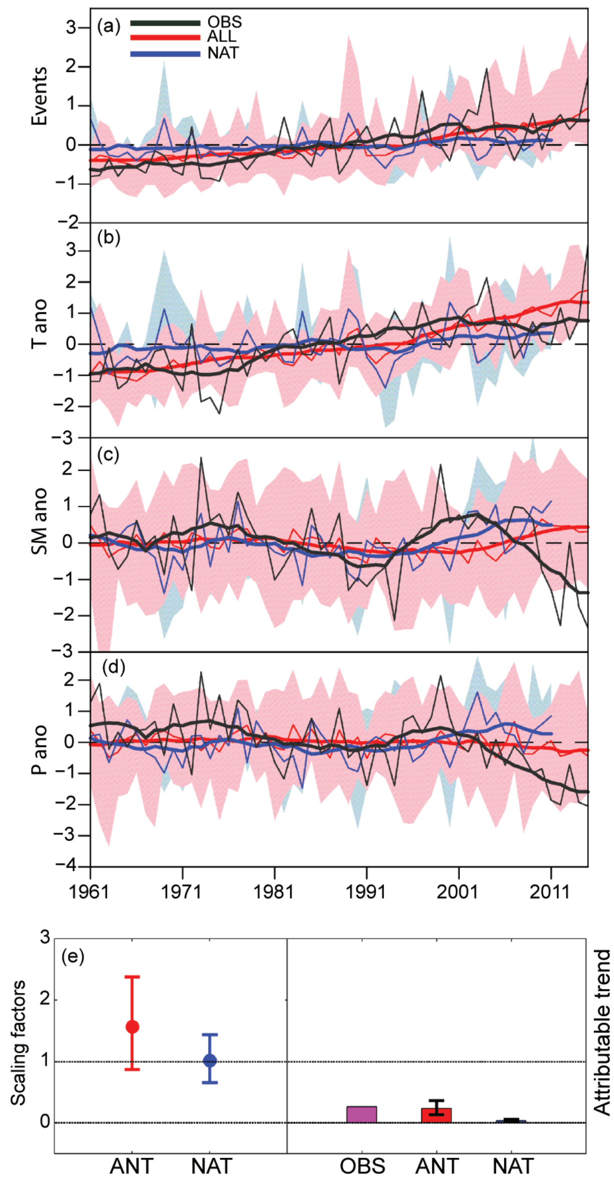

Fig. 17.2. Observed and simulated anomalies of (a) flash drought events (Events), (b) surface air temperature (T), (c) soil moisture (SM), and (d) precipitation (P) averaged over SA. Results from each CMIP5/VIC simulation were first standardized before constructing the ensemble mean ALL (red lines) and NAT (blue lines). The offline VIC simulations (black lines) were also standardized. (a)–(d) The thick lines are 10-year running means, and the pink and cyan shading display the ranges of ALL and NAT simulations respectively. (e) Best estimates of the scaling factors (left axis) and attributable increasing trend (right axis) from two-signal (ANT = ALL-NAT and NAT) analyses of SA flash drought for the period of 1961–2012. Error bars indicate their corresponding 5%–95% uncertainty ranges estimated via Monte Carlo simulations.

the Public Interest (GYHY201506001), CAS Key Research Program of Frontier Sciences (QYZDY-SSW-DQC012), and Thousand Talents Program for Distinguished Young Scholars.

REFERENCES

Allen, M. R., and P. A. Stott, 2003: Estimating signal amplitudes in optimal fingerprinting. Part I: Theory. *Climate Dyn.*, **21**, 477–491, doi:10.1007/s00382-003-0313-9.

Chen, M., W. Shi, P. Xie, V. B. S. Silva, V. E. Kousky, R. W. Higgins, and J. E. Janowiak, 2008: Assessing objective techniques for gauge-based analyses of global daily precipitation. *J. Geophys. Res.*, **113**, D04110, doi:10.1029/2007JD009132.

Dai, A., 2013: Increasing drought under global warming in observations and models. *Nat. Climate Change*, **3**, 52–58, doi:10.1038/nclimate1633.

Dee, D. P., and Coauthors, 2011: The ERA-Interim reanalysis: Configuration and performance of the data assimilation system. *Quart. J. Roy. Meteor. Soc.*, **137**, 553–597, doi:10.1002/qj.828.

Driver, P., and C. J. C. Reason, 2017: Variability in the Botswana High and its relationship with rainfall and temperature characteristics over southern Africa. *Int. J. Climatol.*, **37**, 570–581, doi:10.1002/joc.5022.

Hoell, A., C. Funk, T. Magadzire, J. Zinke, and G. Husak, 2015: El Niño–Southern Oscillation diversity and Southern Africa teleconnections during Austral Summer. *Climate Dyn.*, **45**, 1583–1599, doi:10.1007/s00382-014-2414-z.

——, ——, J. Zinke, and L. Harrison, 2016: Modulation of the Southern Africa precipitation response to the El Niño Southern Oscillation by the subtropical Indian Ocean Dipole. *Climate Dyn.*, **48**, 2529–2540, doi:10.1007/s00382-016-3220-6.

Hoerling, M. P., J. Eischeid, A. Kumar, R. Leung, A. Mariotti, K. Mo, S. Schubert, and R. Seager, 2014: Causes and predictability of the 2012 Great Plains drought. *Bull. Amer. Meteor. Soc.*, **95**, 269–282, doi:10.1175/BAMS-D-13-00055.1.

Liang, X., E. F. Wood, and D. P. Lettenmaier, 1996: Surface soil moisture parameterization of the VIC-2L model: Evaluation and modifications. *Global Planet. Change*, **13**, 195–206, doi:10.1016/0921-8181(95)00046-1.

Manatsa, D., C. H. Matarira, and G. Mukwada, 2011: Relative impacts of ENSO and Indian Ocean dipole/zonal mode on east SADC rainfall. *Int. J. Climatol.*, **31**, 558–577, doi:10.1002/joc.2086.

Mazdiyasni, O., and A. AghaKouchak, 2015: Substantial increase in concurrent droughts and heatwaves in the United States. *Proc. Natl. Acad. Sci. USA*, **112**, 11 484–11 489, doi:10.1073/pnas.1422945112.

Mo, K. C., and D. P. Lettenmaier, 2015: Heat wave flash droughts in decline. *Geophys. Res. Lett.*, **42**, 2823–2829, doi:10.1002/2015GL064018.

Mueller, B., and S. I. Seneviratne, 2012: Hot days induced by precipitation deficits at the global scale. *Proc. Natl. Acad. Sci. USA*, **109**, 12 398–12 403, doi:10.1073/pnas.1204330109.

Nicholson, S., and D. Entekhabi, 1986: The quasi-periodic behavior of rainfall variability in Africa and its relationship to the southern oscillation. *Arch. Meteor. Geophys. Bioclimatol. A.*, **34**, 311–348, doi:10.1007/BF02257765.

Ratnam, J. V., S. K. Behera, Y. Masumoto, and T. Yamagata, 2014: Remote effects of El Niño and Modoki events on the austral summer precipitation of southern Africa. *J. Climate*, **27**, 3802–3815, doi:10.1175/JCLI-D-13-00431.1.

Reason, C. J. C., 2001: Subtropical Indian Ocean SST dipole events and southern African rainfall. *Geophys. Res. Lett.*, **28**, 2225–2227, doi:10.1029/2000GL012735.

——, and D. Jagadheesha, 2005: A model investigation of recent ENSO impacts over southern Africa. *Meteor. Atmos. Phys.*, **89**, 181–205, doi:10.1007/s00703-005-0128-9.

Sheffield, J., and E. F. Wood, 2008: Projected changes in drought occurrence under future global warming from multi-model, multi-scenario, IPCC AR4 simulations. *Climate Dyn.*, **31**, 79–105, doi:10.1007/s00382-007-0340-z.

——, and Coauthors, 2014: A drought monitoring and forecasting system for sub-Sahara African water resources and food security. *Bull. Amer. Meteor. Soc.*, **95**, 861–882, doi:10.1175/BAMS-D-12-00124.1.

Sun, Y., X. Zhang, F. W. Zwiers, L. Song, H. Wan, T. Hu, H. Yin, and G. Ren, 2014: Rapid increase in the risk of extreme summer heat in Eastern China. *Nat. Climate Change*, **4**, 1082–1085, doi:10.1038/nclimate2410.

Taylor, K. E., R. J. Stouffer, and G. A. Meehl, 2012: An overview of CMIP5 and the experiment design. *Bull. Amer. Meteor. Soc.*, **93**, 485–498, doi:10.1175/BAMS-D-11-00094.1.

Trenberth, K. E., A. Dai, G. van der Schreier, P. D. Jones, J. Barichivich, K. R. Briffa, and J. Sheffield, 2014: Global warming and changes in drought. *Nat. Climate Change*, **4**, 17–22, doi:10.1038/nclimate2067.

Wang, L., X. Yuan, Z. Xie, P. Wu, and Y. Li, 2016: Increasing flash droughts over China during the recent global warming hiatus. *Sci. Rep.*, **6**, 30571, doi:10.1038/srep30571.

Washington, R., and A. Preston, 2006: Extreme wet years over southern Africa: Role of Indian Ocean sea surface temperatures. *J. Geophys. Res.*, **111**, D15104, doi:10.1029/2005JD006724.

Yuan, X., E. F. Wood, N. W. Chaney, J. Sheffield, J. Kam, M. Liang, and K. Guan, 2013: Probabilistic seasonal forecasting of African drought by dynamical models. *J. Hydrometeor.*, **14**, 1706–1720, doi:10.1175/JHM-D-13-054.1.

——, Z. Ma, M. Pan, and C. Shi, 2015: Microwave remote sensing of short-term droughts during crop growing seasons. *Geophys. Res. Lett.*, **42**, 4394–4401, doi:10.1002/2015GL064125.